

**Contents of this file:**

Figures S2 to S5.

**Additional Supporting Information (files uploaded separately):**

**Figure S1:** An animation showing the dominant cycle at each site by decade from 1890 to 2020. Note the slow systematic movement of the ~20-yr cycle (red) southwest over time.

**Introduction**

This Supporting Information contains additional figures referred to in the body of the text. The methods used to generate them are the same as outlined in the paper.

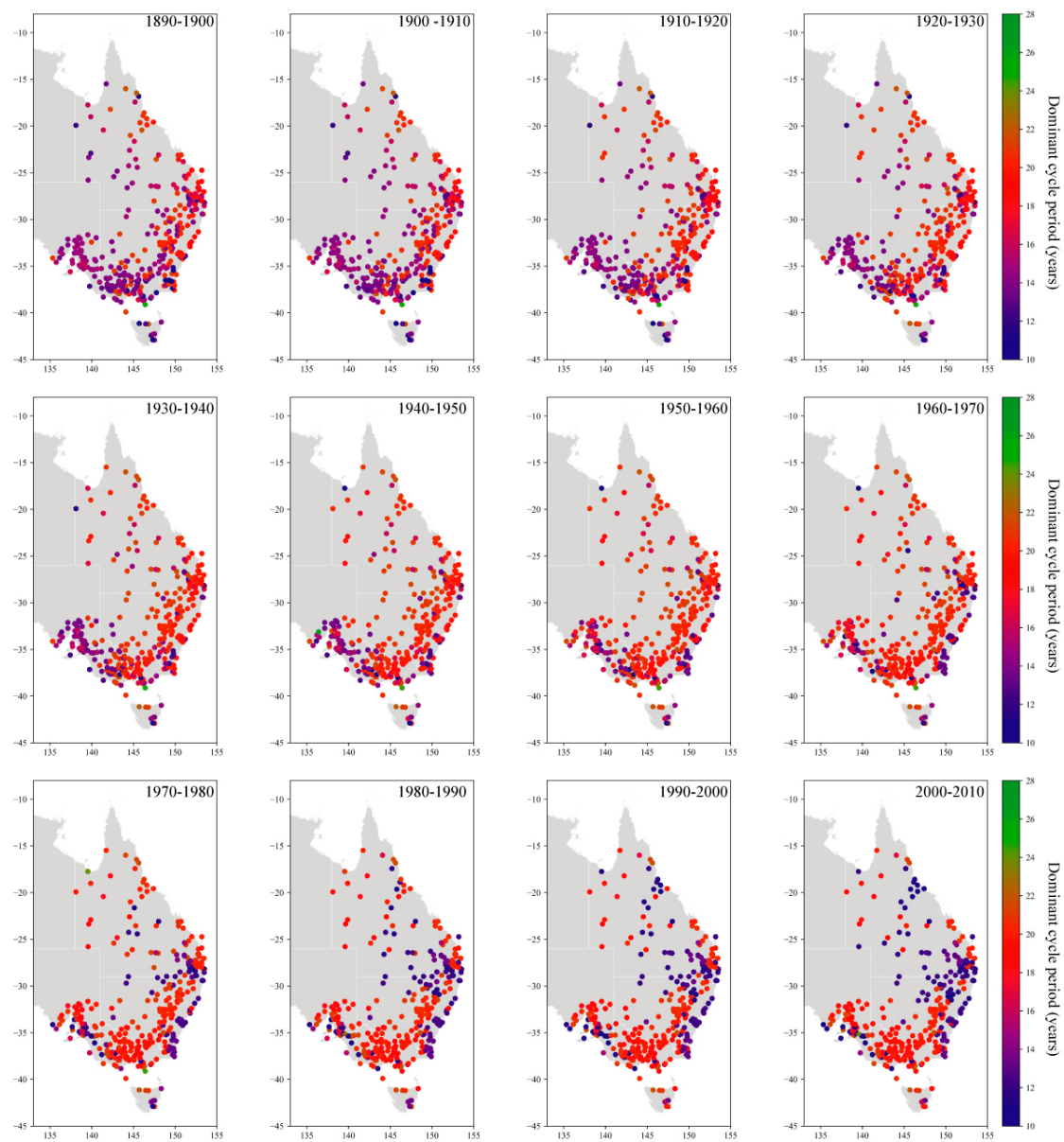


**Figure S2.** Full set of decades testing the significance for the dominant cycle at each individual site for each decade referred to in Figure 6. The sites circled in white are those where the dominant cycle is significantly above the background red noise spectrum at the 95% confidence level.

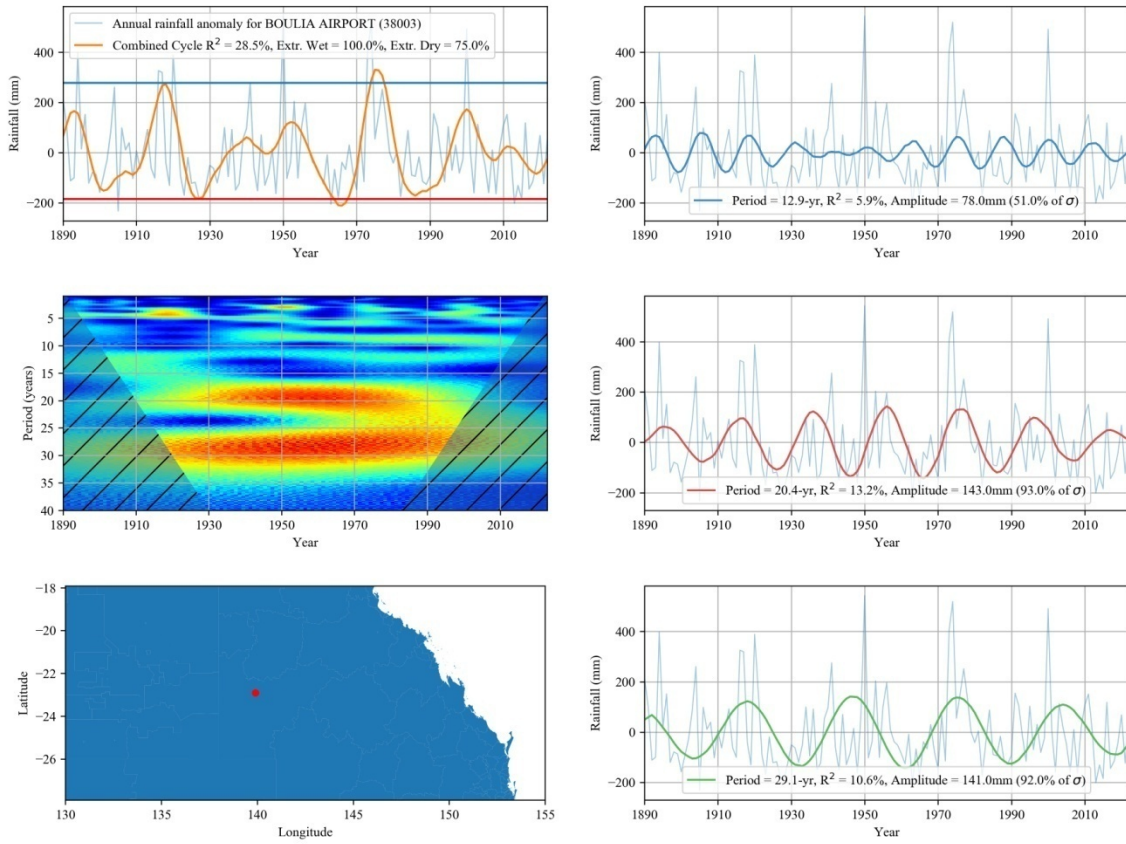


**Figure S3.** The reconstruction analysis for the station with the highest  $R^2$  of all sites tested (28.5%). The high value representing the particularly strong influence of the 20.4-yr and 29.1-yr cycles - both with an amplitude/ $\sigma$  ratio of over 90%.

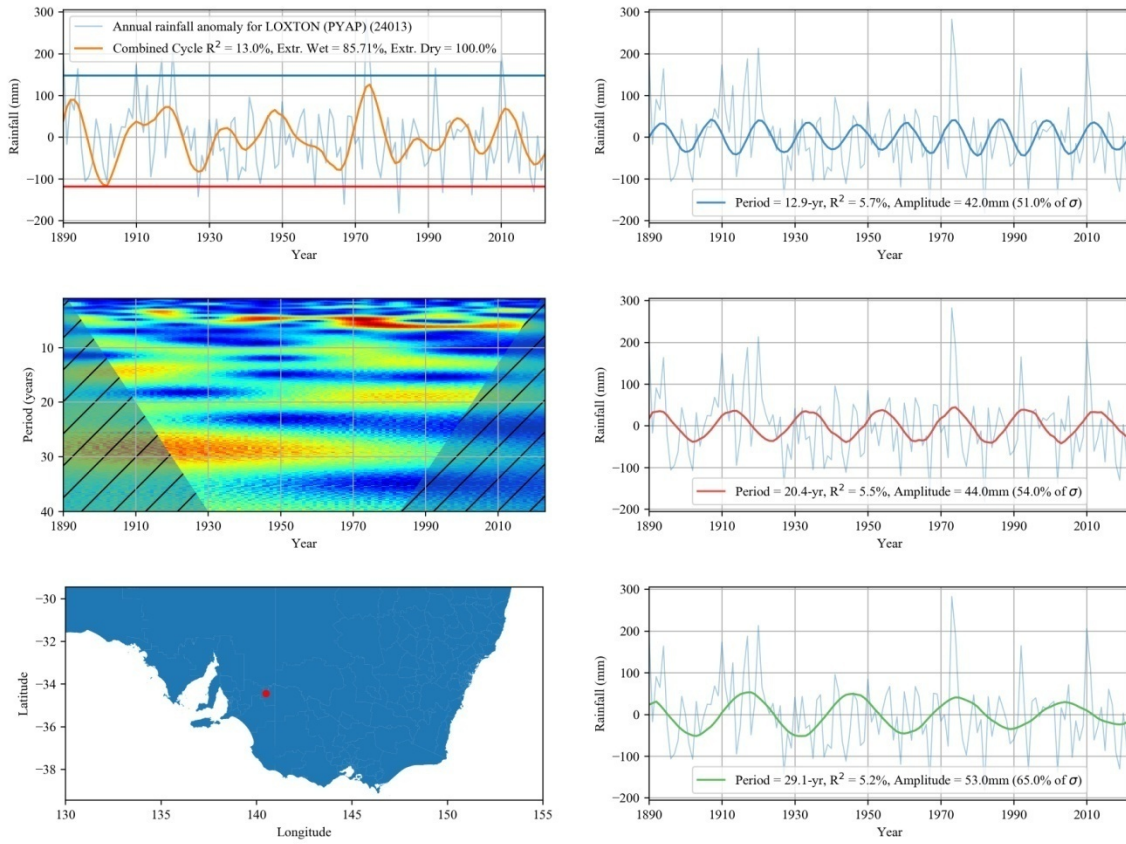


**Figure S4.** The reconstruction analysis for the station reflecting the mean  $R^2$  of all sites tested (13%). Influence of all three cycles is relatively even, accounting for 5-6% of rainfall variance and 50-65% of amplitude/ $\sigma$ .

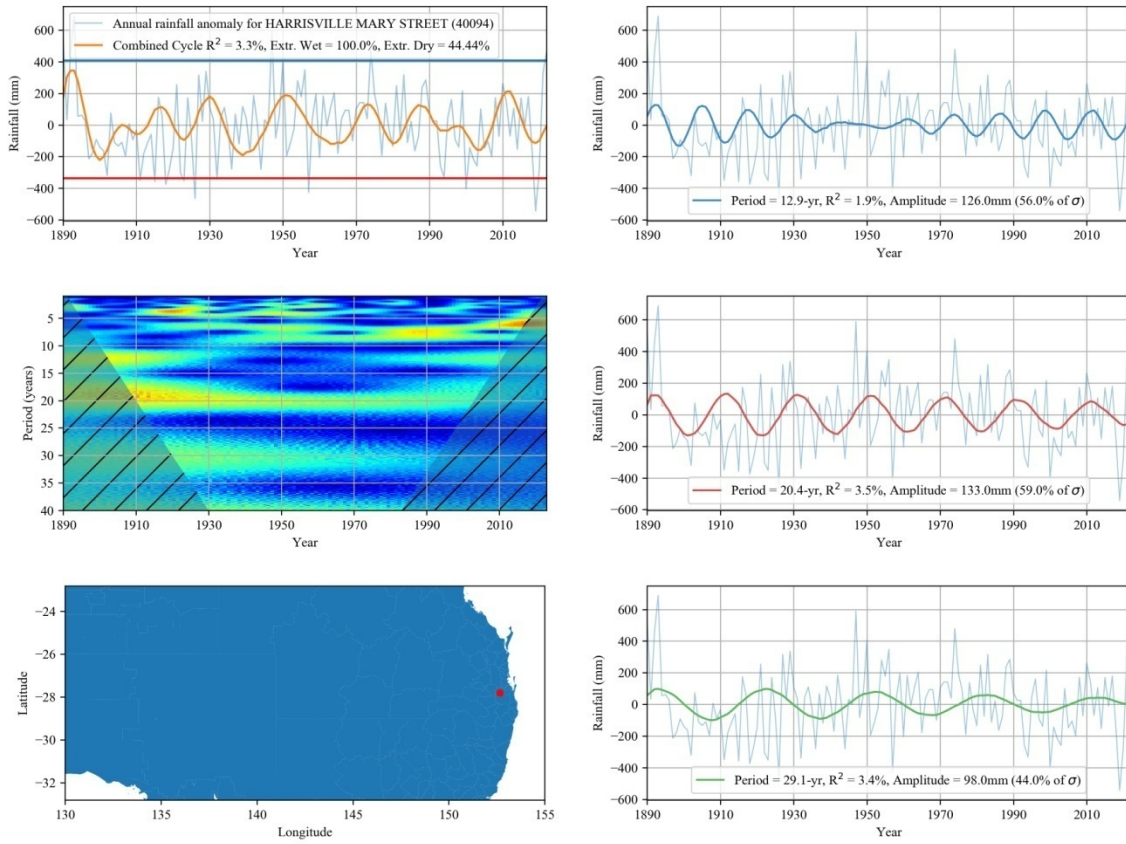


**Figure S5.** The reconstruction analysis for the station reflecting the lowest  $R^2$  of all sites tested (3.3%). The wavelet spectrum shows all 3 cycles are still present at the site, but their influence is relatively weak. The 20.4-yr is the most consistent, with the 12.9-yr cycle almost disappearing entirely between 1940 and 1960.